

The **next generation** GBCA  
from Guerbet is here

Explore new possibilities >

Guerbet | 

© Guerbet 2024 GUOB220151-A

# AJNR

## **Discrepancy Between Neuroimaging Findings and Clinical Phenotype in Alexander Disease**

A. Dinopoulos, J.R. Gorospe, J.C. Egelhoff, K.M. Cecil, P.  
Nicolaidou, P. Morehart and T. DeGrauw

*AJNR Am J Neuroradiol* 2006, 27 (10) 2088-2092  
<http://www.ajnr.org/content/27/10/2088>

This information is current as  
of July 23, 2024.

# Discrepancy Between Neuroimaging Findings and Clinical Phenotype in Alexander Disease

## CASE REPORT

A. Dinopoulos  
J.R. Gorospe  
J.C. Egelhoff  
K.M. Cecil  
P. Nicolaidou  
P. Morehart  
T. DeGrauw

**SUMMARY:** We present a case of infantile-onset Alexander disease (AD) with a novel glial fibrillary acidic protein mutation but without clinical evidence of neurologic deterioration. Brain MRI studies showed typical AD findings and increasing size of frontal cavitations. Serial proton MR spectroscopy demonstrated high levels of myo-inositol and lactic acid and decreasing levels of *N*-acetylaspartate. The degree of demyelination and the timing of the axonal degeneration may determine phenotypic severity of the disease. Conventional neuroimaging techniques cannot always predict the outcome.

Alexander disease (AD) is a rare progressive neurologic disorder occurring primarily in infants and children. In decreasing order of frequency, 3 forms of Alexander disease are recognized on the basis of the age of onset: infantile (birth to 2 years), juvenile (2–12 years), and adult. In infantile AD, the average age of onset is 6 months, and affected infants most frequently present with increasing macrocephaly, failure to thrive, psychomotor delay, seizures, and bulbar dysfunction. In juvenile AD, the age at onset of the symptoms varies from 2 to 14 years, but subtle neurologic signs may be present earlier. Macrocephaly is less consistent in this form, and symptoms include progressive bulbar and pseudobulbar dysfunction, speech difficulties with dysarthria, increasing swallowing problems, and apneic attacks. In adult AD, the onset of symptoms is variable, the clinical features are highly heterogeneous, and the course of the disease is either episodic progressive or slowly progressive.

The most distinctive pathologic feature of AD is the presence of widespread deposition of cytoplasmic inclusions, termed “Rosenthal fibers,” mainly in perivascular, subpial, and subependymal astrocytes.<sup>1,2</sup> A characteristic histologic feature, mainly of the infantile form of AD, is the near-complete absence of myelin sheaths, which is most pronounced in the frontal white matter.<sup>3</sup> In adults, and occasionally in juvenile patients, the pathology may be more limited, involving mainly the brain stem and cerebellum and having relative preservation of the myelin attenuation.<sup>4</sup> An accurate diagnosis of AD is facilitated by a set of MR imaging criteria.<sup>5</sup> The identification of a *de novo* heterozygous mutation on the glial fibrillary acidic protein (*GFAP*) gene, absent in the parents, provides the genetic confirmation of the disease. The development of molecular testing has allowed the recognition of several atypical clinical and imaging phenotypes.<sup>6</sup>

We present a case of infantile-onset AD with typical imaging characteristics but having a surprisingly mild clinical course despite deterioration on neuroimaging. The patient was confirmed to harbor a novel mutation in the *GFAP* gene.

A review of published reports of genetically proved mild infantile cases is also provided.

### Case Report

The index patient is a 5-year-old girl born to nonconsanguineous parents after a full-term uneventful pregnancy. The family history was negative for neurologic illness. At of 3.5 months, she presented with complex partial seizures, and an electroencephalography showed right temporal epileptiform activity. The head circumference at 4 months of age was 42 cm (90th percentile). The seizures initially were controlled with phenobarbital and subsequently with valproic acid. Her initial growth and development were minimally delayed; she sat at 9 months, walked with support at 12 months, and walked unsupported at 18 months and had 5–6 words by 24 months. On the most recent examination (5 years of age), her motor abilities were appropriate for her age. She was able to make simple sentences, but her expressive language was delayed. An attempt to taper antiepileptics was unsuccessful, and since then, she has had excellent seizure control on valproic acid. She has a relative macrocephaly (weight and height <5th percentile and head circumference 90th percentile). On neurologic examination, cranial nerves were intact, muscle strength and tone were normal, and deep tendon reflexes were brisk. There were no signs of spasticity, ataxia, or dyskinesias.

Extensive laboratory metabolic testing found normal levels of lactate, pyruvate, plasma amino acids, vitamin E, vitamin B<sub>12</sub>, urine organic acids, very long-chain fatty acids, phytanic acid, and lysosomal enzymes. Findings of an ophthalmologic examination were also normal.

### Neuroimaging and Spectroscopy

The patient had a series of MR imaging performed at of 3.5 months, 8 months, 20 months, and 39 months of age. The last 3 studies were performed in our institution on a 1.5T MR scanner (Signa; GE Healthcare, Milwaukee, Wis). Standard MR imaging was performed that included the following: sagittal T1-weighted, axial T2-weighted, axial fluid-attenuated inversion recovery (FLAIR), coronal fast spin-echo, and coronal FLAIR as well as postgadolinium axial and coronal T1-weighted sequences. Single-voxel proton MR spectroscopy acquired with short and long TEs, 35 and 288 msec, respectively, in the clinical setting used the PROBE-PRESS localization technique (GE Healthcare).

All 4 examinations showed abnormal signal intensity (high T2, FLAIR, and low T1), predominately in the frontal white matter in a symmetric distribution. The arcuate fibers, genu of the corpus callosum, and the external and extreme capsules were involved, whereas

Received November 17, 2005; accepted November 21.

From the Departments of Neurology (A.D., P.M., T.D.) and Radiology (J.C.E., K.M.C.), Cincinnati Children's Hospital Medical Center, Cincinnati, Ohio; the Center for Genetic Medicine, Children's National Medical Center (J.R.G.), Washington, DC; and the Department of Pediatrics (P.N.), Attiko University Hospital, Athens, Greece.

Address correspondence to Argirios Dinopoulos, MD, PhD, Neurology Division, Cincinnati Children's Hospital Medical Centre, 3333 Burnet Ave, Cincinnati, OH 45229-3039; e-mail: argidino@yahoo.com

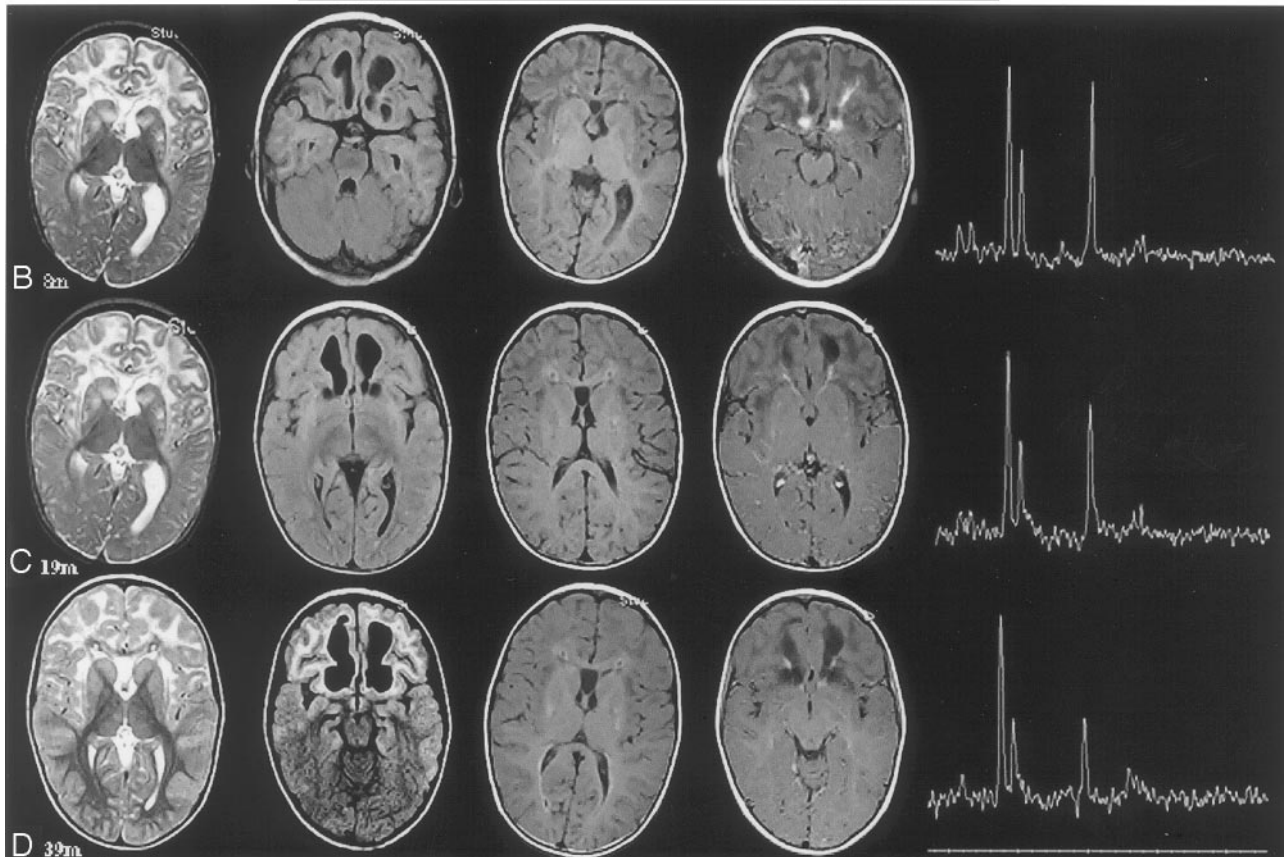
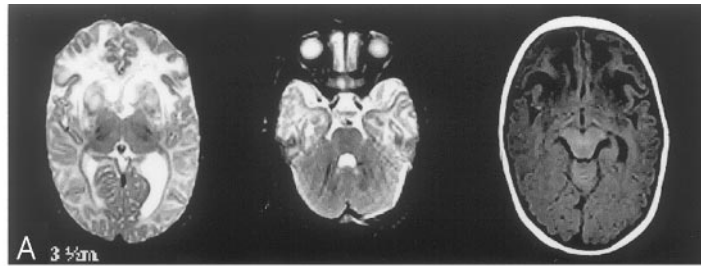


**Fig 1.** The first row (A) shows axial T2- and T1-weighted images, not obtained in our institution, at the age of 3.5 months. The rows B–D represent MR imaging studies (axial T2-weighted, axial FLAIR, axial T1-weighted precontrast, axial T1-weighted postcontrast) and proton MR spectroscopy studies (long-echo TE, 288; with the voxel placed on the left frontal white matter) performed at our institution at the ages of 8 months, 19 months, and 39 months, respectively. White matter signal-intensity abnormality (high T2-weighted, FLAIR, and low T1-weighted) with frontal predominance involving the arcuate fibers and the external and the extreme capsule is apparent in all studies. The white matter has a swollen appearance in all studies except the last one (D). Basal ganglia symmetric signal-intensity abnormality with patchy appearance involving mainly the caudate and putamen (striatum) is apparent in the first 3 studies. The signal intensity is significantly less in the last study (D). Increasing size of the frontal cavitations is apparent with the subsequent studies. A periventricular rim of high intensity is seen on the T1-weighted images of the studies B–D. Contrast enhancement is less apparent in the last study (D). Spectroscopy results are shown on Table 2.

the internal capsules were spared. The frontal white matter at the ages of 3.5 months, 8 months, and 19 months (Fig 1A–C) had a swollen appearance not seen on the MR imaging at the age of 39 months (Fig 1D). A periventricular thin rim of low signal intensity on T2-weighted images and high signal intensity on T1-weighted images were clearly seen on the last 3 MR studies (Fig 1B–D). Symmetric high T2 and FLAIR signal intensity in a patchy distribution was seen in the basal ganglia (mainly the caudate and putamen) on all of the examinations but to a lesser degree on the last examination (Fig 1D). Cavitations of the frontal white matter were present on the first study, and their size increased progressively on subsequent studies. After gadolinium administration (Fig 1B–D), patchy enhancement of the frontal white matter was appreciated mainly adjacent to the cavitations. The enhancement was minimal on the last MR imaging at the age of 39 months (Fig 1D). Brain proton MR spectroscopy acquired within the frontal white matter at 8 months demonstrated abnormally low levels

of *N*-acetylaspartate (NAA), high levels of myo-inositol (mIns), and lactic acid. A comparison of subsequent MR spectroscopy acquisitions, particularly at 8 months versus 39 months, found decreasing NAA and increasing mIns, lactate, and cholines when analyzed by using LC Model software (Stephen Provencher, Oakville, Ontario, Canada).<sup>7</sup> Creatine (Cr), phosphocreatine, and composite glutamate/glutamine concentrations levels were relatively stable. Metabolite concentrations are reported in institutional units because relaxation rates were not measured clinically (Table 1).

#### DNA Analysis

After informed consent was obtained from the patient's parents, genomic deoxyribonucleic acid (DNA) was isolated from peripheral leukocytes by using the protocol provided with the Purigene DNA Isolation Kit (Gentra Systems, Minneapolis, Minn). The genomic DNA was used in polymerase chain reactions (PCR) designed to am-

**Table 1: Spectroscopy results**

Age	Echo		Cr &				Echo	
	Time 1	NAA	PCr	Cho	mIns	Glx	Time 2	Lactate
8 months	35	3.9	4.6	1.5	6.0	7.7	288	2.7
19 months	35	3.6	4.3	1.6	6.1	7.6	288	3.3
39 months	35	1.7	4.3	1.9	7.7	7.6	288	4.4

**Note:**—Concentrations are reported in institutional units (IU). *N*-acetylaspartate (NAA), creatine and phosphocreatine (Cr & PCr), choline (Cho), myo-inositol (mIns), glutamate/glutamine (Glx) concentration values are reported from the spectroscopy acquired at an echo time of 35 ms from the left frontal white matter. Lactate concentration values are reported from the spectroscopy acquired at an echo time of 288 ms from the left frontal white matter. Acquisitions used a repetition time of 2000 ms.

plify the entire coding region and exon-intron boundaries of *GFAP* (GenBank accession no. XM 008388). Both strands of the resulting PCRs were sequenced by using the ABI 3100 automated sequencer (Applied Biosystems, Weiterstadt, Germany). A C to T base change corresponding to nucleotide 1087 (1087c→t) was detected in exon 6 of 1 of the patient's *GFAP* alleles. This base change causes a change from an alanine to a valine at amino acid residue #358 (A358V). Both parents tested negative for the presence of the 1087c→t mutation (Fig 2).

### Discussion

We present a case of infantile onset AD demonstrating extensive and progressive neuroimaging characteristics of the disease but a very mild clinical phenotype. The patient harbors a novel mutation in *GFAP* gene (A358V) that was not identified in the parents, indicating that this *de novo* mutation is responsible for the patient's condition.

MR imaging is capable of suggesting the diagnosis of AD with substantial accuracy, as demonstrated by the high correlation between the presence of the MR imaging criteria and the presence of *de novo* *GFAP* gene mutations. The neuroimaging studies of our patient fulfill 4 of the 5 MR imaging criteria: 1) extensive cerebral white matter changes with frontal predominance, 2) periventricular rim of high T1-weighted signal intensity, 3) abnormal signal intensity in the basal ganglia, and

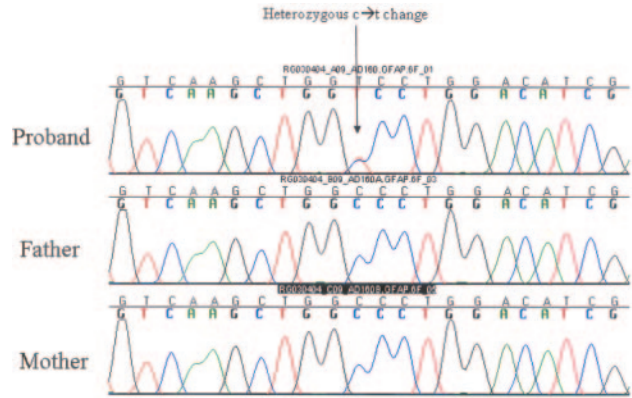


**Fig 2.** Sequencing chromatograms show the C to T base change corresponding to nucleotide 1087 (1087c→t) that was detected on the patient's *GFAP* alleles. Both parents tested negative for the presence of the 1087c→t mutation.

4) contrast enhancement of the frontal white matter. Furthermore, prominent cavitations of the frontal white matter, with increasing size with time, were seen as early as 3.5 months of age. MR imaging abnormalities typical for AD have been previously described in mild infantile and even in asymptomatic AD cases (Table 2). It appears that there is not a direct correlation between the neuroimaging abnormalities and the clinical phenotype, though the presence of cavitations is more often associated with the severe phenotype.<sup>8</sup>

It is difficult to explain the discrepancy between the dramatic MR imaging picture of extensive white matter involvement and cavitations and the mild symptoms. This observation points to the limitation of the conventional MR imaging to define the underlying pathology. Discrepancy between neuroimaging findings and clinical symptoms is seen in other leukoencephalopathies such as in megalencephaly leukoencephalopathy with subcortical cysts (MLC) and in the leukoencephalopathy associated with the congenital muscular dystrophy (CMD). Particu-

**Table 2: Features of the clinical, neuroimaging, and genetic characteristics of cases of infantile onset Alexander disease associated with mild clinical phenotype**

Mutation	Sex	Age		Macrocephaly	Seizures	Spasticity	Bulbar signs	Cognitive impairment	MRI	Reference
		Presentation	Follow-up							
R79C 235 c → t	1*	F	7 m	19 y	+	+	+	-	T	6
	2*	M	3 m	14 y	-	-	-	-	T	17
	3*	M	11 m	7 y	-	+	-→+	-	-→+	T
R79H 250 g → a	4†		0 m	7.5 y	-	+	-→+	-	-→+	T
	5†		6 m	20 y	-	+	-→+	-	-→+	T
	6†		6 m	4.7 y	-	+	-	-	-	T
	7†	F	12 m	8 y	-	-	-	-	-	T
R88C 276 c → t	8*	M	Asymptomatic	at 4 y	-	-	-	-	-	T
	9*	M	Asymptomatic	at 3 y	+	-	-	-	-	T
	10*		6 m	3.5 y	-	-	-	-	-	T
L90P 283 c → t	11†§	F	5 m	5.9 y	-	+	-→+	-	-→+	T
	12†	M	8 m	8 y	+	+	-	+	+	T
R239C 716 c → t	13¶		18 m	8 y	-	+	-→+	-	-→+	T
	14¶§	M	<12 m	8 y	-	-	-	+	-	A
A253G 758 g → t	15¶§	M	1 m	-	-	-	-	-	-	A
	16¶§	M	Asymptomatic	-	-	-	-	-	-	T
L331P 1006 c → t	17¶§	F	Asymptomatic	at 7 y	-	-	-	-	-	A
	18†	F	3 m	5 y	+	+	-	-	-	T
R416W 1260 c → t	19*	M	Asymptomatic	at 11 y	-	-	-	-	-	T

**Note:**—\* indicates previously proven pathogenic mutation; †, absence of the mutation in both parents; ¶, absence of the mutation in one parent; §, absence of the mutation in healthy control subjects; m, months; y, years; †, presence; -, absence; T, typical; A, atypical.

larly in MLC, the vacuolization within the myelin is responsible for the white matter appearance on the MR imaging, whereas the preservation of the myelin sheath counts for the mild clinical symptoms.<sup>9</sup> In both MLC and CMD, a blood-brain barrier dysfunction is speculated,<sup>10</sup> which may also be true for AD, given that the Rosenthal fibers are mainly localized in astrocytic end-feet, which are part of the barrier.<sup>11</sup>

AD, a primary disorder of the astrocytes and the demyelination, particularly apparent in the infantile form, is a result of disturbed myelin maintenance due to aberrant interactions between astrocytes and oligodendrocytes.<sup>12,13</sup> Despite the extensive demyelination, at least initially, the axons appear intact, and when axonal degeneration occurs, it is less dramatic than the myelin loss. It is not clear when the axonal degeneration begins and which factors determine this process during the evolution of the AD pathology. It is possible that the degree and timing of the axonal degeneration determines the phenotypic severity and the age of symptom onset.

Clinical heterogeneity is not uncommon in AD; and patients without macrocephaly, patients with less severe course, and even asymptomatic patients discovered incidentally have been described.<sup>14</sup> Table 2 shows the clinical and genetic characteristics of patients with a mild infantile as well as asymptomatic AD. In some of these cases, the initial normal psychomotor development was subsequently followed by a progressive neurologic impairment, suggesting an ongoing neurodegenerative process.<sup>15</sup> Hence, the clinician needs to exercise caution when making prognostic statements. In the index patient, the decreasing NAA concentration levels on subsequent proton MR spectroscopy raises the concern of a subclinical neuronal degeneration that may become clinically apparent with time.

All forms of AD are caused by de novo *GFAP* mutations producing a dominant gain of function of the *GFAP* protein that exerts a toxic effect on astrocyte function. Our patient's mutation is located near the end of the 2B helical region (Fig 3). At the same location, other mutations associated with severe infantile and mild juvenile phenotype are clustered, suggesting that the location of the mutation alone cannot determine the severity of the disease. A genotype-phenotype correlation is discerned for certain mutations (R79 mutations appearing much less severe than those of R239), which implies that certain mutations may be less deleterious on astrocytes than others. However, mutations with a wide phenotypic variability have been described such as R416W mutation, which can cause all 3 forms of the disease.<sup>13,16</sup> It is apparent that although a *GFAP* gene mutation is the underlying cause of AD, additional genetic or environmental factors can modify the final phenotype. One asymptomatic patient with the R416W mutation and a P47 L amino acid change on the *GFAP* gene has been reported, suggesting that certain polymorphisms might alter the progression of the disease.<sup>13,14</sup>

The clinical and neuroimaging phenotype of AD has been expanded significantly and clinicians must be aware of this variability. Apart from the typical forms of AD, several atypical presentations. Axonal preservation, as a result of less deleterious mutations or other genetic modifications, may be an explanation of the milder phenotype. MR imaging can docu-

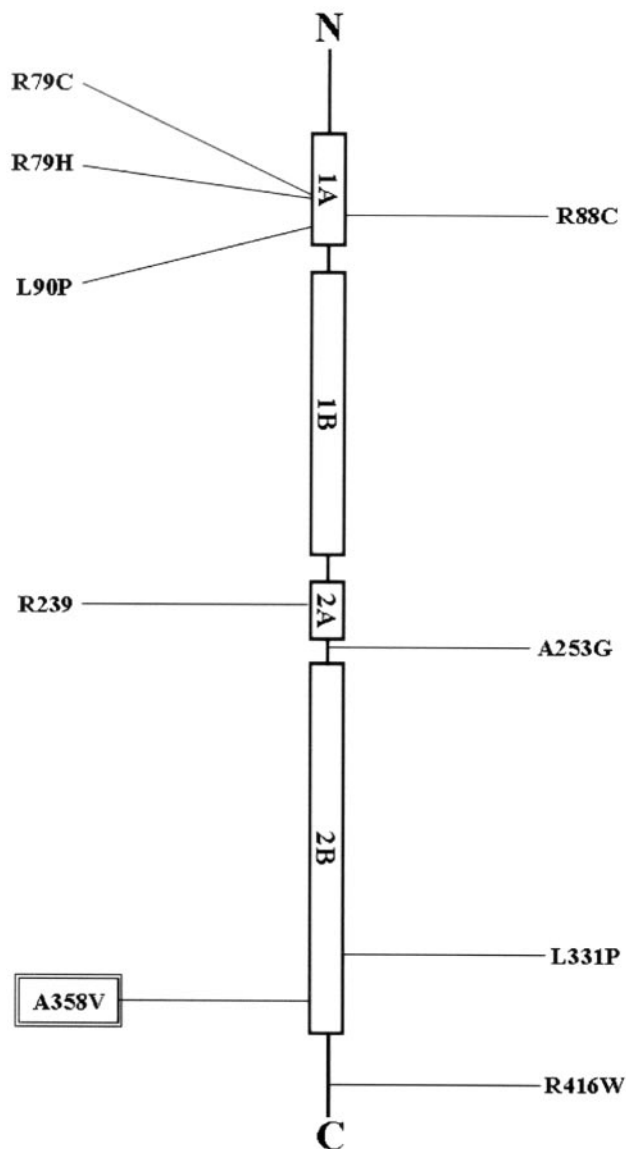


**Fig 3.** The figure depicts the location of each of the mild AD-associated mutations in *GFAP*, in relation to the protein domain structure of intermediate filaments. The protein has a central rod domain that is subdivided into 4  $\alpha$ -helical subdomains separated by nonhelical areas.

ment the extent of demyelination. Nevertheless, it cannot ascertain the condition of axonal integrity, and it cannot always predict the severity and the course of the disease. Proton MR spectroscopy may be a better prognostic tool, but further studies are warranted.

## References

- Soffer D, Horoupian DS. Rosenthal fibers formation in the central nervous system: its relation to Alexander's disease. *Acta Neuropathol (Berl)* 1979;47: 81–84
- Towfighi J, Young R, Sassani J, et al. Alexander's disease: further light- and electron-microscopic observations. *Acta Neuropathol (Berl)* 1983;61:36–42
- van der Knaap MS, Valk J. Alexander Disease. In: *Magnetic Resonance of Myelination and Myelin Disorders*. 3rd ed. Berlin, Germany: Springer-Verlag; 2005: 416–35
- Spalke G, Mennel HD. Alexander's disease in an adult: clinicopathologic study of a case and review of the literature. *Clin Neuropathol* 1982;1:106–12
- van der Knaap MS, Naidu S, Breiter SN, et al. Alexander disease: diagnosis with MR imaging. *AJNR Am J Neuroradiol* 2001;22:541–52
- van der Knaap MS, Salomons GS, Li R, et al. Unusual variants of Alexander's disease. *Ann Neurol* 2005;57:327–38

7. Provencher SW. **Estimation of metabolite concentrations from localized in vivo proton NMR spectra.** *Magn Reson Med* 1993;30:672–79
8. Klein EA, Anzil AP. **Prominent white matter cavitation in an infant with Alexander's disease.** *Clin Neuropathol* 1994;13:31–38
9. van der Knaap MS, Barth PG, Vrensens GF, et al. **Histopathology of an infantile-onset spongiform leukoencephalopathy with a discrepantly mild clinical course.** *Acta Neuropathol (Berl)* 1996;92:206–12
10. Boor PK, de Groot K, Waisfisz Q, et al. **MLC1: a novel protein in distal astroglial processes.** *J Neuropathol Exp Neurol* 2005;64:412–19
11. Mignot C, Boespflug-Tanguy O, Gelot A, et al. **Alexander disease: putative mechanisms of an astrocytic encephalopathy.** *Cell Mol Life Sci* 2004;61:369–85
12. Messing A, Goldman JE, Johnson AB, et al. **Alexander disease: new insights from genetics.** *J Neuropathol Exp Neurol* 2001;60:563–73
13. Li R, Messing A, Goldman JE, et al. **GFAP mutations in Alexander disease.** *Int J Dev Neurosci* 2002;20:259–68
14. Gorospe JR, Naidu S, Johnson AB, et al. **Molecular findings in symptomatic and pre-symptomatic Alexander disease patients.** *Neurology* 2002;58:1494–500
15. Rodriguez D, Gauthier F, Bertini E, et al. **Infantile Alexander disease: spectrum of GFAP mutations and genotype-phenotype correlation.** *Am J Hum Genet* 2001;69:1134–40
16. Li R, Johnson AB, Salomons G, et al. **Glial fibrillary acidic protein mutations in infantile, juvenile, and adult forms of Alexander disease.** *Ann Neurol* 2005;57:310–26
17. Brenner M, Johnson AB, Boespflug-Tanguy O, et al. **Mutations in GFAP, encoding glial fibrillary acidic protein, are associated with Alexander disease.** *Nat Genet* 2001;27:117–20
18. Guthrie SO, Burton EM, Knowles P, et al. **Alexander's disease in a neurologically normal child: a case report.** *Pediatr Radiol* 2003;33:47–49
19. Suzuki Y, Kanazawa N, Takenaka J, et al. **A case of infantile Alexander disease with a milder phenotype and a novel GFAP mutation, L90P.** *Brain Dev* 2004;26:206–08
20. Shiihara T, Sawaishi Y, Adachi M, K, et al. **Asymptomatic hereditary Alexander's disease caused by a novel mutation in GFAP.** *J Neurol Sci* 2004;225:125–27